COMPUTATIONAL & APPLIED MATHEMATICS

Volume 28, N. 3, pp. 259–275, 2009

ISSN 0101-8205
www.scielo.br/cam

On the statistical steady state gas-solid flow in a riser as predicted through a two-fluid simulation

CHRISTIAN C. MILIOLI and FERNANDO E. MILIOLI

Thermal and Fluids Engineering Laboratory
EESC – School of Engineering of São Carlos, USP – University of São Paulo
Av. Trabalhador São-Carlense, 400, 13566-590 São Carlos, SP, Brazil

E-mails: ccosta@sc.usp.br / milioli@sc.usp.br

Abstract. This work is concerned with the extremely high computational costs of the two-fluid simulations of gas-solid flows in risers. In a previous article [1] a procedure was proposed to speed up the simulations towards the desired statistical steady state flow regime. In this continuing article the concern is turned to the time extent that a simulation must advance inside the statistical steady state regime so that suitable time averaged predictions can be made. An analysis is carried out using the results of a transient two-fluid simulation of a riser flow performed inside the statistical steady state regime. Time averaged results were produced considering different time averaging intervals of 5, 10, 15 and 20 seconds. Both the transient behavior of the predictions and the time averaged results are discussed. For the present case, it was found that 10 seconds of fluidization taken inside the statistical steady state regime are enough for a reasonable qualitative description of the average flow.

Mathematical subject classification: Primary: 06B10; Secondary: 06D05.

Key words: two-fluid simulation, gas-solid flow, circulating fluidized bed, riser.

1 Introduction

Circulating fluidized bed reactors are widely used in large scale applications such as catalytic cracking of petrol and coal combustion. Development and

#CAM-29/08. Received: 16/X/08. Accepted: 15/VIII/09.
The first author is supported by CNPq.

design in those areas are strongly based on demonstration plants, at extremely high costs. In this context, treatments applying computational fluid mechanics assume considerable relevance. The complex gas-solid flow patterns which develop inside the risers of circulating fluidized bed reactors determine reaction rates, so that rigorous hydrodynamic descriptions are required. The continuum Eulerian or two-fluid models are currently considered the most practical choice for providing such descriptions [2].

Owing to flow instabilities, the risers can not operate in real steady state conditions. Instead, they operate in pseudo-permanent or statistical steady state flow regimes, imposing numerical simulations to be transient. Figure 1 illustrates the behavior of any parameter as predicted from a two-fluid transient simulation of the gas-solid flow in risers (see [3], for instance). From a given initial condition, the simulation goes through an early stage, and finally reaches the so called statistical steady state regime. For practical purposes, this regime is considered to be reached when all the flow parameters start to oscillate around well defined averages.

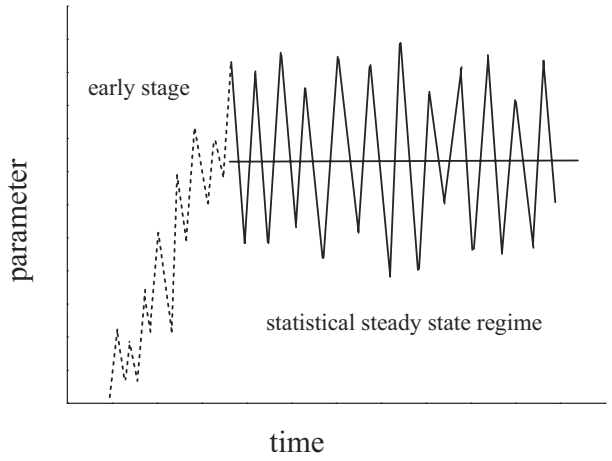

Figure 1 – Behavior of any parameter as predicted from a two-fluid transient simulation.

Most of the literature reported works on two-fluid simulation of risers only present time averaged data, mainly for comparisons to experiment. Only a few works are reported which also present results on the transient behavior of the flow, including data on both the early stage and the statistical steady state

regime [3-8]. None of those works performed any analysis on the averaging time interval that would be required for obtaining suitable averaged results. Tsuo and Gidaspow [8] generated time averaged results considering only 5 seconds of real fluidization inside the statistical steady state regime, Zhang and Vander-Heyden [7] considered 10 to 15 seconds, Mathiesen et al. [6] considered 16 to 20 seconds, and Cabezas-Gómez and Milioli [5] considered 80 seconds.

Despite the lack of information regarding the required time interval for accurate averaging, its determination is very significant having in view the very excessive computing times characteristic of two-fluid simulations of risers. It is known that usual simulations can easily take months of CPU processing time. In a matter of fact, months may well be required only for overcoming the early stage of a simulation. Zhang and VanderHeyden [7] took 101 days of CPU processing to provide 21 seconds of real fluidization. About a third of those days was spent only overcoming the early stage. If the statistical steady state regime is to be accurately simulated, a real time advance numerical procedure must be applied. Noting that no precise results are required for the early stage, this step may be simulated by applying a distorted time numerical advance. Of course, the distorted time advance is not expected to lead to any convergence since the flow never reaches a true steady state regime. However, the iterative marching on distorted time allows the solution to quickly overcome the early stage and reach a point where a real time advance simulation may be engaged. As the simulation is switched from distorted time to real time advance, converged predictions are found which are generated directly inside the statistical steady state regime. A discussion on this matter can be found in Milioli and Milioli [1], where it is shown that, for a particular case, the above procedure saved about 230 days of wall clock processing which would be required for simulating the early stage alone. It should be noted that, while the previous distorted time step procedure affects the following real time transient solution, the averages inside the statistical steady state regime shall be unaffected, unless numerical instabilities develop throughout the distorted time numerical advance. In the present simulation no numerical instabilities were observed. In this work, predictions are produced inside the statistical steady state regime following the above procedure. Time averaged results are derived for different time intervals. Then, a

discussion is carried out on the independence of the averaged results regarding the averaging time interval. The present simulation was performed in a 10 nodes Beowulf cluster of PCs, each one with 2 processors Intel Xeon 3.06 GHz and 20 Gb Ram, totalizing 122.4 Gflops of computing capacity.

2 Two-fluid modeling of gas-solid flow

Two-fluid conservative equations are based on the major hypotheses of continuum and thermodynamic equilibrium commonly applied in fluid mechanics. Two-fluid models for multi-phase flows, including gas-solid flows, are developed from integral mass and momentum balances over suitable control volumes comprising all the phases (see [9-12], for instance). The theorems of Leibniz and Gauss are applied to the integral balances giving rise to local instantaneous conservative equations for each phase and jump conditions describing interface interactions among phases. Then, averaging procedures are applied for providing averaged equations. The interfaces among phases in multiphase dispersed flows like the gas-solid fluidized flow are defined around a huge number of particles, and are highly dynamical and chaotic. Because of that, local instantaneous formulations become inapplicable. The averaging procedures are used to go around such difficulty. Different averaging procedures may be applied like volume averaging, time averaging and ensemble or statistical averaging. Those procedures are usually assumed equivalent (ergodicity hypothesis). Closure laws are required to deal with parameters and coefficients present in the average conservative equations, and boundary and initial conditions must be set. The closure laws provide correlations and data for viscous stress tensors, viscosities, pressures and drag. All the phases are commonly assumed to be Newtonian-Stokesian fluids. Pressure and viscosities of solid phases are generally accounted for through either semi-empirical or theoretical correlations. An interface drag force, empirically correlated, accounts for the interface momentum transfer between the gas and the solid phases. Wall boundary conditions for the solid phase are determined considering either no-slip, free slip or partial slip conditions. For the gas phase the conventional no-slip condition is applied. Following the above, two different formulations have been applied by most of the researchers. In the first, conservative equations are directly generated for

each phase. In the second formulation, conservative equations are generated for the gas phase and for the mixture. From those equations, conservative equations are derived for the solid phase. Gidaspow [11] named those formulations as models A and B, respectively. The formulation of model A, which is used in this work, is showed next.

Gas phase continuity:

$$\frac{\partial(\alpha_g \rho_g)}{\partial t} + \overrightarrow{\nabla} \cdot (\alpha_g \rho_g \overrightarrow{U_g}) = 0 \tag{1}$$

Solid phase continuity:

$$\frac{\partial(\alpha_s \rho_s)}{\partial t} + \overrightarrow{\nabla} \cdot (\alpha_s \rho_s \overrightarrow{U_s}) = 0 \tag{2}$$

Gas phase momentum:

$$\begin{aligned} &\frac{\partial(\alpha_g \rho_g \overrightarrow{U_g})}{\partial t} + \overrightarrow{\nabla} \cdot (\alpha_g \rho_g \overrightarrow{U_g} \overrightarrow{U_g}) = \\ &-\overrightarrow{\nabla}(\alpha_g P_g) + \overrightarrow{\nabla} \cdot (\alpha_g \overline{\overline{\tau_g}}) + \alpha_g \rho_g \overrightarrow{F_g} + \beta(\overrightarrow{U_s} - \overrightarrow{U_g}) \end{aligned} \tag{3}$$

Solid phase momentum:

$$\begin{aligned} &\frac{\partial(\alpha_s \rho_s \overrightarrow{U_s})}{\partial t} + \overrightarrow{\nabla} \cdot (\alpha_s \rho_s \overrightarrow{U_s} \overrightarrow{U_s}) = \\ &-\overrightarrow{\nabla}(\alpha_s P_s) + \overrightarrow{\nabla} \cdot (\alpha_s \overline{\overline{\tau_s}}) + \alpha_s \rho_s \overrightarrow{F_s} - \beta(\overrightarrow{U_s} - \overrightarrow{U_g}) \end{aligned} \tag{4}$$

Stress tensor for phase k:

$$\overline{\overline{\tau_k}} = \mu_k[\overrightarrow{\nabla} \overrightarrow{U_k} + (\overrightarrow{\nabla} \overrightarrow{U_k})^T] + \lambda_k(\overrightarrow{\nabla} \cdot \overrightarrow{U_k})\overline{\overline{I}} \tag{5}$$

where, $\mu_k = \text{constant}$, $\lambda_k = \frac{2}{3}\mu_k$.

Solid phase pressure [13]:

$$\overrightarrow{\nabla}(\alpha_s P_s) = -\Omega \overrightarrow{\nabla} \alpha_s + \overrightarrow{\nabla}(\alpha_s P_g) \tag{6}$$

where,

$$\Omega = \exp[-20(\alpha_g - 0.62)] \tag{7}$$

Volumetric continuity:

$$\alpha_g + \alpha_s = 1 \tag{8}$$

External body forces per unit mass:

$$\overrightarrow{F_g} = \overrightarrow{g} \tag{9}$$

$$\overrightarrow{F_s} = \left(\frac{\rho_s - \rho_g}{\rho_s}\right)\overrightarrow{g} \tag{10}$$

Equations of state: $\rho_g = \text{constante}$, $\rho_s = \text{constante}$.

Interface drag [11]:

$$\beta = 150\frac{\alpha_s^2 \mu_g}{\alpha g (d_p \varphi_s)^2} + 1.75\frac{\rho_g \alpha_s |v_g - v_s|}{(d_p \varphi_s)} \quad \text{for } \alpha_s > 0.2 \tag{11}$$

$$\beta = \frac{3}{4} C_{D_s} \frac{\rho_g \alpha_s \alpha_g |v_g - v_s|}{(d_p \varphi_s)} \alpha_g^{-2.65} \quad \text{for } \alpha_s \leq 0.2 \tag{12}$$

where:

$$C_{D_s} = \frac{24}{\mathrm{Re}_p \left(1 + 0.15\ \mathrm{Re}_p^{0.687}\right)} \quad \text{for } \mathrm{Re}_p < 1000 \tag{13}$$

and

$$C_{D_s} = 0.44 \quad \mathrm{Re}_p \geq 1000 \tag{14}$$

with

$$\mathrm{Re}_p = \frac{|v_g - v_s|\, d_p \rho_g \alpha_g}{\mu_g} \tag{15}$$

The symbols in Equations (1) to (15) stand for: C_D – drag coefficient, non-dimensional; d_p – particle diameter, m; $\overrightarrow{F}$ – external body force per unit mass, N; $\overrightarrow{g}$ – gravity acceleration, m/s^2; $\overline{\overline{I}}$ – unit tensor; P – pressure, N/m^2; Re_p – Reynolds number, non-dimensional; t – time, s; $\overrightarrow{U}$ – average velocity vector, m/s; u, v, w – velocity components in the directions, m/s; α – volume fraction, m$_k^3$/m^3; β – gas-solid friction coefficient, kg/m^{3}s; φ_s – particle shape factor, non-dimensional; λ – bulk viscosity, Ns/m^2; μ – dynamic viscosity, Ns/m^2; ρ – density, kg/m^3; $\overline{\overline{\tau}}$ – viscous stress tensor, N/m^2; Ω – particle-particle elasticity modulus, N/m^2; g – gas phase; k – either, gas or solid phases; s – solid phase.

Equations (11), (12), and (13)-(14) are due to Ergun [14], Wen and Yu [15] and Rowe [16], respectively. The complex set of partial differential non-linear coupled equations of the two-fluid models can only be solved through numerical procedures. In this work, the numerical model available in the software CFX [17-19] is used. An element-based finite volume discretization method is followed. Non-structured meshes are applied in Cartesian coordinate system. Tetrahedral mesh elements are used. The median method is applied to define control volumes over which the conservative equations are integrated to obtain the discretized equations. The discretization of convective terms are performed through a second order high resolution interpolation scheme. The discretization of diffusive and other terms is performed through the second order central differencing scheme. Time discretization is performed through a first order interpolation scheme. The discretized equations are solved implicitly through a direct method applying matrix inversion. As a consequence, couplings such as pressure $\times$ velocity, and drag, are straightly solved, and iteration is only required to overcome non-linearities.

3 Simulation

The present simulation was performed for hydrodynamic conditions which have already been considered by other authors, and are typical of circulating fluidized bed coal combustion. The solid mass flux of 24.9 kg/m^{2}s, particulate size of 520 μm, and the reactor size (height of 5.56 m and width of 7.62 cm) were taken from Luo [20]. Figure 2 shows the three-dimensional cylindrical geometry that was assumed, and a sample of the numerical mesh that was applied.

Table 1 brings fluid and particulate properties, initial and boundary conditions, and numerical settings. The dynamic viscosity of the solid phase of 0.509 N/m^{2}s was determined by Tsuo [21] using the empirical data of Luo [20].

4 Results and Discussion

Figures 3 to 6 show results of the distorted time non-converged predictions for the early stage, as well as the following real time converged predictions for the statistical steady state stage of the simulation.

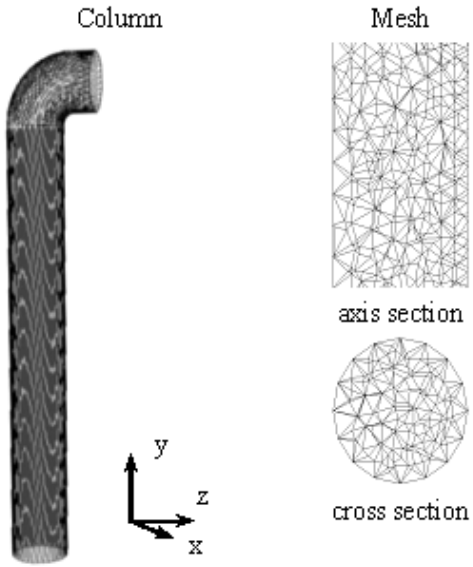

Figure 2 – Geometry and a sample of the tetrahedral numerical mesh.

The results stand for the transient behavior of the gas and solid axial velocities, solid mass flux and solid volume fraction, averaged over the cross section at 3.4 m above entrance. The distorted time predictions were allowed to proceed up to 45.454 seconds of distorted time fluidization. All the graphs show that, from about 20 seconds of distorted time fluidization, the predictions were already oscillating around well defined time averages, indicating that the early stage of the simulation was overcome.

Following the 45.454 seconds of non-converged distorted results, 20 seconds of real time predictions are presented, which are converged inside a rms (root mean square) of 1×10^{-5} s.

All the graphs show that the real time predictions oscillate around well defined time averages right from the beginning, showing that the real time simulation was completely developed inside the statistical steady state regime. Of course, there is a quantitative difference among time averages taken inside the distorted time and the real time intervals, since the predictions in the first interval lack precision. The distorted time predictions are quite imprecise since not converged. Otherwise, the real time predictions are precise inside the imposed rms.

Column	
Diameter = 7.62 cm	Height = 5.56 m
Particulate size = 520μm	
Solid mass flux (G_s) = 24.9 kg/m^{2}s	
Phases	
g = air at 300 K	s = glass beads at 300 K
Properties	
$\rho_g = 1.1614$ kg/m^3	$\rho_s = 2620$ kg/m^3
$\mu_g = 1.8210^{-5}$ N/m^{2}s	$\mu_s = 0.509$ N/m^{2}s
$W_g = 28.97$ kg/kmol	$W_s = 60$ kg/kmol
Boundary conditions	
Inlet	
$u_g = 0$ m/s	$u_s = 0$ m/s
$v_g = 4.979$ m/s	$v_s = 0.386$ m/s
$w_g = 0$ m/s	$w_s = 0$ m/s
$\alpha_g = 0.9754$ m$_g^3$/m^3	$\alpha_s = 0.0246$ m$_s^3$/m^3
outlet	walls
Locally parabolic	$g =$ no-slip
$P_g = 15880$ N/m^2	$s =$ free-slip
Initial conditions (distorted time run)	
As in the inlet, except:	
$\alpha_g = 0.62$ m$_g^3$/m^3	$\alpha_s = 0.38$ m$_s^3$/m^3
Numerical settings	
Mesh	
Tetrahedrals = 206229	
Average edge length = 9.4 mm	
Nodes = 42029	
rms for convergence = 1×10^{-5} s	
Distorted time step = 1×10^{-3} s	
Real time step = 1×10^{-4} s	

Table 1 – Properties, initial and boundary conditions, and numerical settings.

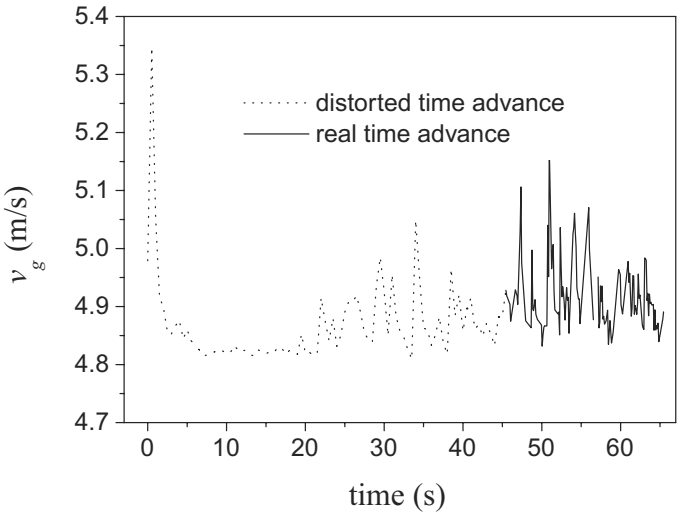

Figure 3 – Transient behavior of the gas axial velocity averaged over the cross section at 3.4 m above entrance, for the distorted time simulation followed by the real time simulation.

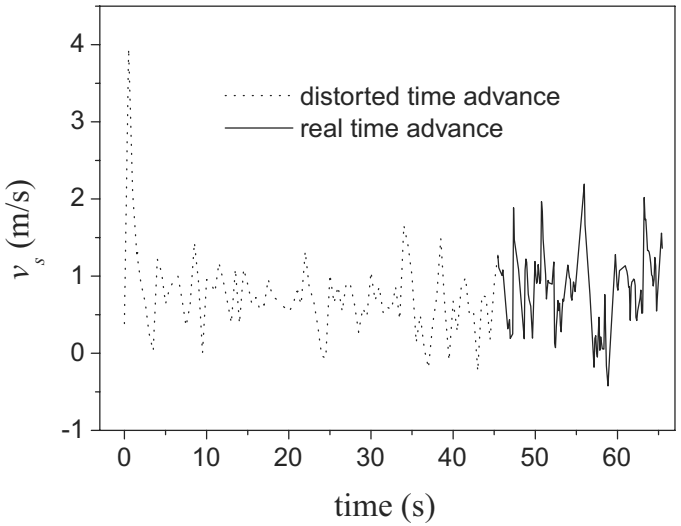

Figure 4 – Transient behavior of the solid axial velocity averaged over the cross section at 3.4 m above entrance, for the distorted time simulation followed by the real time simulation.

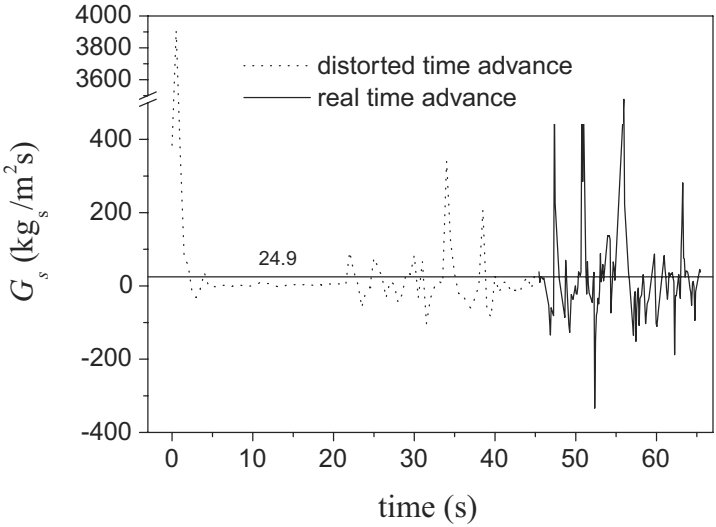

Figure 5 – Transient behavior of the solid mass flux averaged over the cross section at 3.4 m above entrance, for the distorted time simulation followed by the real time simulation.

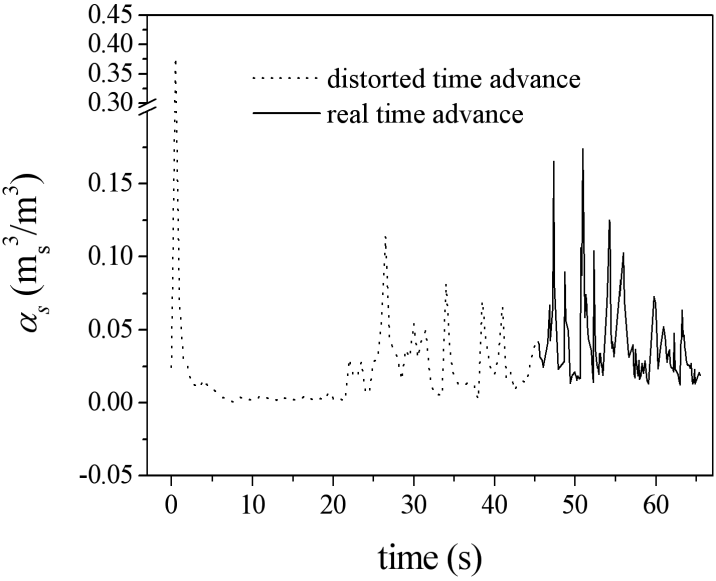

Figure 6 – Transient behavior of the solid volume fraction averaged over the cross section at 3.4 m above entrance, for the distorted time simulation followed by the real time simulation.

Time averaged results were generated for the predictions inside the statistical steady state region, considering different averaging intervals. Those were 0-5, 0-10, 0-15, and 0-20 seconds. Figures 7 to 10 show those results, which are time averaged profiles of gas and solid axial velocities, solid mass flux and solid volume fraction, through the diameter of the column, in the cross section at 3.4 m above entrance. Time averaged results in vertical risers are expected to be symmetric. The only possible cause for asymmetry, in the present case, concerns the asymmetric exit section. As the exit is very far away from the section where the results are analysed, it could be argued that only slight asymetries should be observed. However, the formation of clusters at the walls close to the exit, and the following down flow along the walls resulted highly affected by the asymetric exit, accounting for the asymmetric profiles reported in Figures 7 to 10.

For all of the concerning parameters, it is seen that the time averaging interval significantly affected the averaged predictions as well as the symmetry of the profiles. The differences were not only quantitative, but also qualitative. This is particularly clear for the profiles of solid mass flux showed in Figure 9. For the time interval (0-5s) the profile resulted quite asymmetric, unlike the nearly symmetric profiles obtained for the intervals (0-10s), (0-15s) and (0-20s).

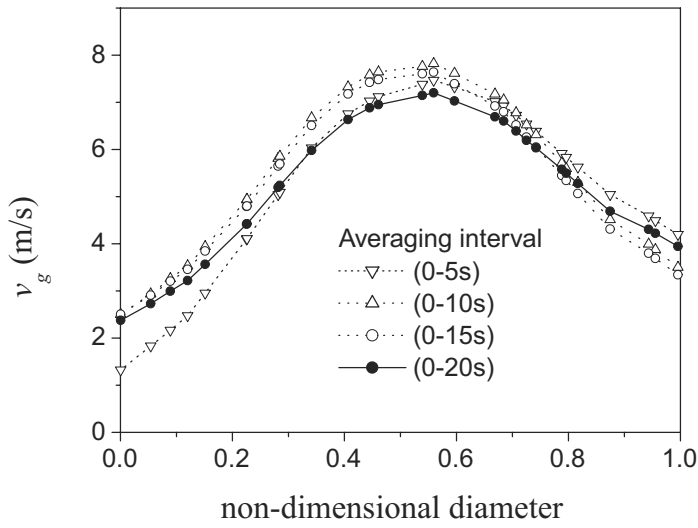

Figure 7 – Time averaged profiles of gas axial velocity through the diameter of the column, in the cross section at 3.4 m above entrance, for different time intervals.

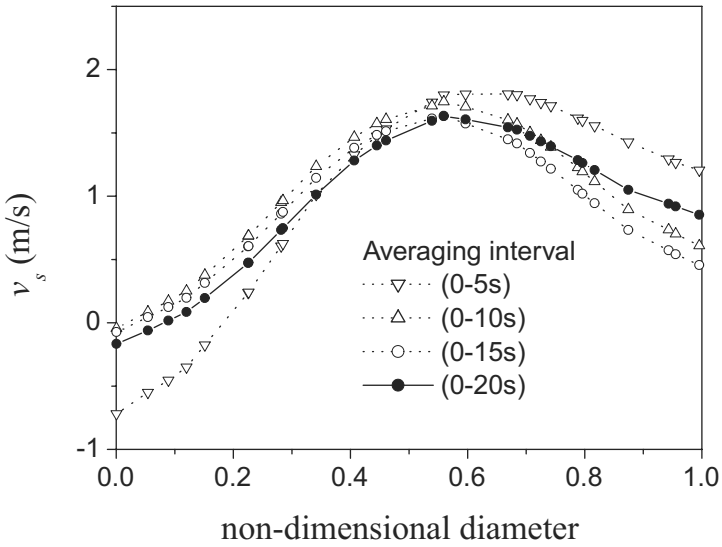

Figure 8 – Time averaged profiles of solid axial velocity through the diameter of the column, in the cross section at 3.4 m above entrance, for different time intervals.

It was expected that the profiles for all of the parameters became closer as the time averaging interval was raised.

This, however, only happened for some of the parameters (solid mass flux and volume fraction). Otherwise, for each one of the parameters, the profiles presented the same qualitative behavior for time averaging intervals of 10 seconds and higher. Figure 11 shows axial profiles of solid volume fraction averaged both in time and through the cross section of the column. All of the profiles, for the different time intervals, show the expected behavior. The solid volume fraction and its axial gradient are higher at the bottom, decaying with height as expected. Also, the solid concentration slightly increases at exit owing to a stronger formation of clusters at this spot. There are considerable differences among the results for the different time averaging intervals. However, all of the predictions presented the same qualitative behavior.

5 Conclusions

A two-fluid transient simulation was performed for the gas-solid flow in a riser of circulating fluidized bed. Time averaged results were derived for different

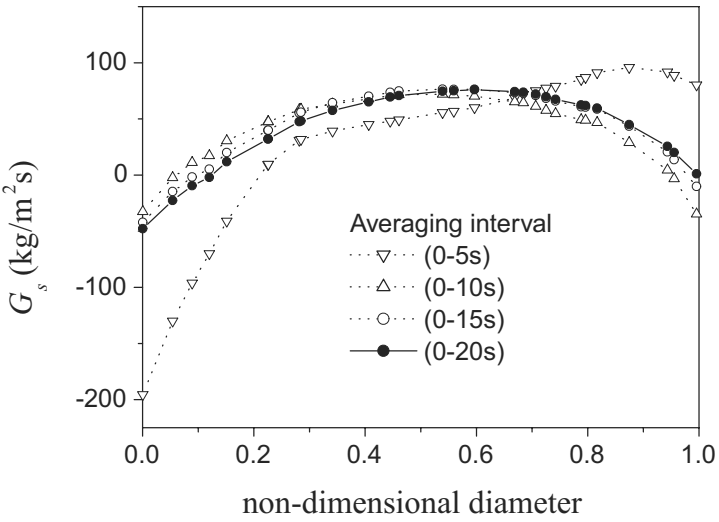

Figure 9 – Time averaged profiles of solid mass flux through the diameter of the column, in the cross section at 3.4 m above entrance, for different time intervals.

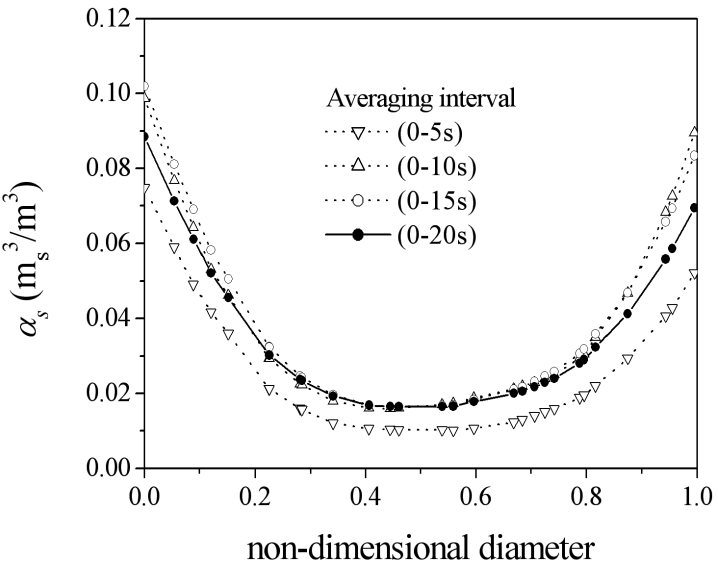

Figure 10 – Time averaged profiles of solid volume fraction through the diameter of the column, in the cross section at 3.4 m above entrance, for different time intervals.

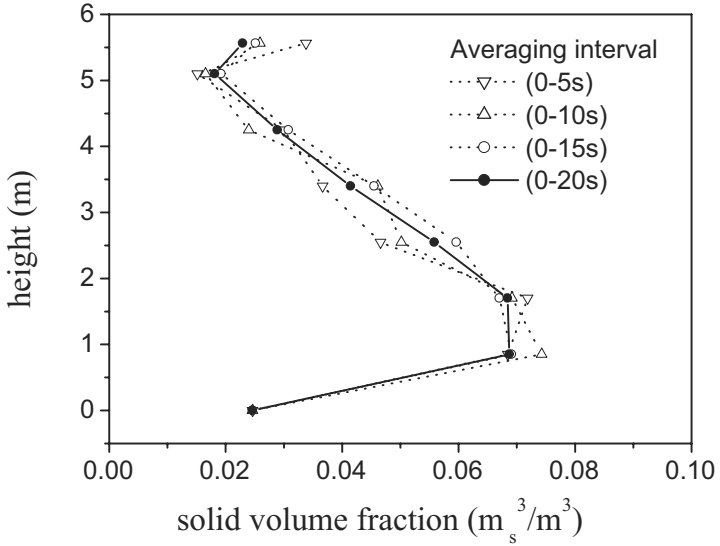

Figure 11 – Axial profiles of solid volume fraction averaged both in time and through the cross section of the column, for different time averaging intervals.

time intervals inside the statistical steady state regime. The considered time intervals were (0-5s), (0-10s), (0-15s) and (0-20s). The present results were not conclusive as far as a more rigorous quantitative analysis is concerned. It became clear that such an assessment only would be possible if a longer simulation time was available. Thereby, the independence of the predictions regarding the time averaging interval could not be addressed rigorously. However, it was shown that a time averaging interval of 10 seconds was enough for reasonable qualitative analyses. This achievement is of considerable importance having in view the huge computational costs typical of two-fluid simulations of gas-solid flows in risers. The 20 seconds of real fluidization analyzed in the present work were generated in about 480 days of wall clock processing in a cluster of PCs using 20 cores Intel Xeon 3.06 MHz. This extremely high computational cost strongly suggests that the minimum time interval required for representative analysis should be rigorously established. Finally, it must be stressed that the present analysis was performed having in view a unique simulation, for a unique set of operational conditions. The present conclusions are, of course, not to be generalized.

Acknowledgements. This work was supported by The National Council for Scientific and Technological Development (CNPq).

REFERENCES

[1] C.C. Milioli and F.E. Milioli, *Reaching the statistical steady state regime in two-fluid simulation of risers*. Powder Technology, **167** (2006), 26–32.

[2] S. Sundaresan, *Modeling the hydrodynamics of multiphase flow reactors: current status and challenges*. American Institute of Chemical Engineers Journal, **46** (2000), 1102–1105.

[3] K. Agrawal, P.N. Loezos, M. Syamlal and S. Sundaresan, *The role of meso-scale structures in rapid gas-solid flows*. Journal of Fluid Mechanics, **445** (2001), 151–185.

[4] A.T. Andrews IV, P.N. Loezos and S. Sundaresan, *Coarse-grid simulation of gas-particle flows in vertical risers*. Industrial and Engineering Chemistry Research, **44** (2005), 6022–6037.

[5] L. Cabezas-Gómez and F.E. Milioli, *Numerical study on the influence of various physical parameters over the gas-solid two-phase flow in the 2D riser of a circulating fluidized bed*. Powder Technology, **132** (2003), 216–225.

[6] V. Mathiesen, T. Solberg and B.H. Hjertager, *Predictions of gas/particle flow with an Eulerian model including a realistic particle size distribution*. Powder Technology, **112** (2000), 34–45.

[7] D.Z. Zhang and W.B. Van der Heyden, *High-resolution three-dimensional numerical simulation of a circulating fluidized bed*. Powder Technology, **116** (2001), 133–141.

[8] Y.P. Tsuo and D. Gidaspow, *Computation of flow patterns in circulating fluidized beds*. American Institute of Chemical Engineers Journal, **36** (1990), 885–896.

[9] T.B. Anderson and R. Jackson, *Fluid mechanical description of fluidized beds. Equations of motion*. Industrial and Engineering Chemistry Fundamentals, **6** (1967), 527–539.

[10] M. Ishii, *Thermo-fluid dynamic theory of two-phase flow*. Eyrolles, Paris (1975).

[11] D. Gidaspow, *Multiphase flow and fluidization*. Academic Press, San Diego, CA (1994).

[12] H. Enwald, E. Peirano and A.-E Almsted, *Eulerian two-phase flow theory applied to fluidization*. International Journal of Multiphase Flow, **22** (1999), 21–66.

[13] D. Gidaspow and B. Ettehadieh, *Fluidization in two-dimensional beds with a jet. Part II. Hydrodynamic modeling*. Industrial and Engineering Chemistry Fundamentals, **22** (1983), 193–201.

[14] S. Ergun, *Fluid flow through packed columns*. Chemical Engineering Progress, **48** (1952), 89–94.

[15] C.Y. Wen and Y.U. Yu, *Mechanics of fluidization*. Chemical Engineering Progress Symposium Series, **62** (1966), 100–111.

[16] P.N. Rowe, *Drag forces in a hydraulic model of a fluidized bed. Part II*. Transactions of the Institute of Chemical Engineers, **39** (1961), 175–180.

[17] CFX5.7, *Multiphase flow theory, Solver theory manual*. Ansys Canada, Ontario (2004).

[18] CFX5.7, *Multiphase flow modelling, Solver modelling manual*. Ansys Canada, Ontario (2004).

[19] CFX5.7, *Discretization and solution theory, Solver theory manual*. Ansys Canada, Ontario (2004).

[20] K.M. Luo, *Experimental gas-solid vertical transport*. PhD Thesis, Illinois Institute of Technology, Chicago, Illinois (1987).

[21] Y.P. Tsuo, *Computation of flow regimes in circulating fluidized beds*. PhD thesis, Illinois Institute of Technology, Chicago, Illinois (1989).